

MIT Open Access Articles

Constraining a Thin Dark Matter Disk with Gaia

The MIT Faculty has made this article openly available. **Please share** how this access benefits you. Your story matters.

Citation: Schutz, Katelin, et al. "Constraining a Thin Dark Matter Disk with Gaia." *Physical Review Letters*, vol. 121, no. 8, Aug. 2018. © 2018 American Physical Society

As Published: <http://dx.doi.org/10.1103/PhysRevLett.121.081101>

Publisher: American Physical Society

Persistent URL: <http://hdl.handle.net/1721.1/117666>

Version: Final published version: final published article, as it appeared in a journal, conference proceedings, or other formally published context

Terms of Use: Article is made available in accordance with the publisher's policy and may be subject to US copyright law. Please refer to the publisher's site for terms of use.



Constraining a Thin Dark Matter Disk with *Gaia*

Katelin Schutz,^{1,*} Tongyan Lin,^{1,2,3} Benjamin R. Safdi,⁴ and Chih-Liang Wu⁵

¹*Berkeley Center for Theoretical Physics, University of California, Berkeley, California 94720, USA*

²*Theoretical Physics Group, Lawrence Berkeley National Laboratory, Berkeley, California 94720, USA*

³*Department of Physics, University of California, San Diego, California 92093, USA*

⁴*Leinweber Center for Theoretical Physics, Department of Physics, University of Michigan, Ann Arbor, Michigan 48109, USA*

⁵*Center for Theoretical Physics, Massachusetts Institute of Technology, Cambridge, Massachusetts 02139, USA*

 (Received 4 December 2017; revised manuscript received 4 May 2018; published 21 August 2018)

If a component of the dark matter has dissipative interactions, it could collapse to form a thin dark disk in our Galaxy that is coplanar with the baryonic disk. It has been suggested that dark disks could explain a variety of observed phenomena, including periodic comet impacts. Using the first data release from the *Gaia* space observatory, we search for a dark disk via its effect on stellar kinematics in the Milky Way. Our new limits disfavor the presence of a thin dark matter disk, and we present updated measurements on the total matter density in the Solar neighborhood.

DOI: [10.1103/PhysRevLett.121.081101](https://doi.org/10.1103/PhysRevLett.121.081101)

Introduction.—The particle nature of dark matter (DM) remains a mystery in spite of its large abundance in our Universe. Moreover, some of the simplest DM models are becoming increasingly untenable. Taken together, the wide variety of null searches for particle DM strongly motivates taking a broader view of potential models. Many recently proposed models posit that DM is part of a dark sector, containing interactions or particles that lead to nontrivial dynamics on astrophysical scales [1–16]. Meanwhile, the *Gaia* satellite [17] has been observing one billion stars in the local Milky Way (MW) with high-precision astrometry, which will allow for a vast improvement in our understanding of DM substructure in our Galaxy and its possible origins from dark sectors.

In this Letter, we apply the first *Gaia* data release [18] to constrain the possibility that DM can dissipate energy through interactions in a dark sector. Existing constraints imply that the entire dark sector cannot have strong self interactions, since this would lead to deviations from the predictions of cold DM that are inconsistent with cosmological observations [19–22]. However, it is possible that only a subset of the dark sector interacts strongly or that DM interactions are only strong in low-velocity environments [23–25]. In these cases, there is leeway in cosmological bounds and one must make use of smaller scale observables [26,27]. If the DM component can dissipate energy through emission or upscattering (see, e.g., [16,28–35] for examples of mechanisms), then it can cool and collapse to form DM substructure. These interactions could result in a striking feature in our Galaxy: a thin DM disk (DD) [14,15] that is coplanar with the baryonic disk.

A thin DD may be accompanied by a range of observational signatures. For instance, DDs may be responsible for the ~ 30 million year periodicity of comet impacts [36],

the corotation of Andromeda’s satellites [37,38], the point-like nature of the inner Galaxy GeV excess [39,40], the orbital evolution of binary pulsars [41], and the formation of massive black holes [42], in addition to having implications for DM direct detection [43,44]. Typically, a DD surface density of $\Sigma_{\text{DD}} \sim 10 M_{\odot}/\text{pc}^2$ and a scale height of $h_{\text{DD}} \sim 10$ pc are required to meaningfully impact the above phenomena. (A thicker DD with $h_{\text{DD}} \gtrsim 30$ pc can cause periodic cratering [45]; however, a larger surface density $\Sigma_{\text{DD}} \sim 15\text{--}20 M_{\odot}/\text{pc}^2$ is required to be consistent with paleoclimatic constraints [46]).

Here, we present a comprehensive search for a local DD, using tracer stars as a probe of the local gravitational potential. Specifically, we use the *Tycho-Gaia* Astrometric Solution (TGAS) [47,48] catalog, which provides measured distances and proper motions for ~ 2 million stars in common with the *Tycho-2* catalog [49]. Previous work searching for a DD with stellar kinematics used data from the *Hipparcos* astrometric catalog [50] and excluded local surface densities $\Sigma_{\text{DD}} \gtrsim 14 M_{\odot}/\text{pc}^2$ for dark disks with thickness $h_{\text{DD}} \sim 10$ pc [51]. As compared with *Hipparcos*, the TGAS catalog contains ~ 20 times more stars with three-dimensional positions and proper motions within a larger observed volume, which allows for a significant increase in sensitivity. Our analysis also improves on previous work by including a comprehensive set of confounding factors that were previously not all accounted for, such as uncertainties on the local density of baryonic matter and the tracer star velocity distribution. We exclude $\Sigma_{\text{DD}} \gtrsim 6 M_{\odot}/\text{pc}^2$ for $h_{\text{DD}} \sim 10$ pc, and our results put tension on the DD parameter space of interest for explaining astrophysical anomalies [36–42].

Vertical kinematic modeling.—We use the framework developed in Ref. [52] (and extended in Ref. [51]) to

describe the kinematics of TGAS tracer stars in the presence of a DD. This formalism improves upon previous constraints on a DD that did not self-consistently model the profiles of the baryonic components in the presence of a DD [53–57]. These bounds typically compared the total surface density of the Galactic disk, measured from the dynamics of a tracer population above the disk, to a model of the surface density of the baryons based on extrapolating measurements from the Galactic midplane. However, the models did not include the pinching effect of the DD on the distribution of the baryons, which would lower the inferred baryon surface density for fixed midplane density. Instead, Refs. [51,52] consider the dynamics close to the disk and self-consistently model the baryonic components for fixed DD surface density and scale heights. We summarize the key components below.

The phase-space distribution function of stars $f(\mathbf{x}, \mathbf{v})$ in the local MW obeys the collisionless Boltzmann equation. Assuming that the disk is axisymmetric and in equilibrium, the first nonvanishing moment of the Boltzmann equation in cylindrical coordinates is the Jeans equation for population A ,

$$\frac{1}{r\nu_A} \partial_r(r\nu_A\sigma_{A,rz}^2) + \frac{1}{\nu_A} \partial_z(\nu_A\sigma_{A,zz}^2) + \partial_z\Phi = 0, \quad (1)$$

where Φ is the total gravitational potential, ν_A is the stellar number density, and $\sigma_{A,ij}^2$ is the velocity dispersion tensor. The first term in Eq. (1), commonly known as the tilt term, can be ignored near the disk midplane where radial derivatives are much smaller than vertical ones [58]. We assume populations are isothermal (constant $\sigma_{A,zz}^2$) near the Galactic plane [59]. With these simplifying assumptions, the solution to the vertical Jeans equation is $\nu_A(z) = \nu_{A,0}e^{-\Phi(z)/\sigma_A^2}$, where we impose $\Phi(0) = 0$ and define $\sigma_A \equiv \sigma_{A,zz}$. For populations composed of roughly equal mass constituents (including gaseous populations), we then make the assumption that the number density and mass density are proportional, i.e., $\rho_A(z) = \rho_{A,0}e^{-\Phi(z)/\sigma_A^2}$.

We connect the gravitational potential to the mass density of the system with the Poisson equation

$$\nabla^2\Phi = \partial_z^2\Phi + \frac{1}{r} \partial_r(r\partial_r\Phi) = 4\pi G\rho, \quad (2)$$

where ρ is the total mass density of the system. The radial term is related to Oort’s constants, with recent measurements showing $(1/r)\partial_r(r\partial_r\Phi) = (3.4 \pm 0.6) \times 10^{-3} M_\odot/\text{pc}^3$ [60], which can be included in the analysis as a constant effective contribution to the density [61]. Combining the Jeans and Poisson equations under reflection symmetry yields an integral equation. In the limiting case with only one population, the solution is $\rho(z) = \rho_0 \text{sech}^2(\sqrt{2\pi G\rho_0}z/\sigma)$. For multiple populations, the solution for the density profile and Φ must be determined numerically. We use an iterative

solver with two steps per iteration. On the n th iteration, we compute

$$\Phi^{(n)}(z) = 4\pi G \sum_A \int_0^z dz' \int_0^{z'} dz'' \rho_A^{(n)}(z'') \quad (3)$$

and update the density profile for the A th population,

$$\rho_A^{(n+1)}(z) = \rho_{0,A} e^{-\Phi^{(n)}(z)/\sigma_A^2}. \quad (4)$$

Adding more gravitating populations compresses the density profile relative to the single-population case.

Near the midplane, the vertical motion is separable from the other components. For tracers indexed by i , the vertical component of the equilibrium Boltzmann equation is $v_z \partial_z f_i - \partial_z \Phi \partial_{v_z} f_i = 0$, which is satisfied by

$$\nu_i(z) = \nu_{i,0} \int dv_z f_{i,0} \left(\sqrt{v_z^2 + 2\Phi(z)} \right), \quad (5)$$

where $f_{i,0}$ is the vertical velocity distribution at height $z = 0$, normalized to unity. Given $\Phi(z)$, we can then predict the vertical number density profile for a tracer population. In our analysis, we determine $f_{i,0}$ empirically and do not assume that our tracer population is necessarily isothermal.

Mass model.—In order to solve for the gravitational potential, we must have an independent model for the baryons. In Table I, we compile some of the most up-to-date measurements of $\rho_{A,0}$ and σ_A for the local stars and gas, primarily drawing from the results of Ref. [57] and supplementing with velocity dispersions from Refs. [62,63]. The velocity dispersions for gas components are effective dispersions that account for additional pressure terms in the Poisson-Jeans equation. We include uncertainties (measured when available, estimated otherwise) and profile over these nuisance parameters in our analysis.

TABLE I. The baryonic mass model that informs our priors.

Baryonic component	$\rho(0)$ [M_\odot/pc^3]	σ [km/s]
Molecular gas (H_2)	0.0104 ± 0.00312	3.7 ± 0.2
Cold atomic gas [$\text{H}_\text{I}(1)$]	0.0277 ± 0.00554	7.1 ± 0.5
Warm atomic gas [$\text{H}_\text{I}(2)$]	0.0073 ± 0.0007	22.1 ± 2.4
Hot ionized gas (H_II)	0.0005 ± 0.00003	39.0 ± 4.0
Giant stars	0.0006 ± 0.00006	15.5 ± 1.6
$M_V < 3$	0.0018 ± 0.00018	7.5 ± 2.0
$3 < M_V < 4$	0.0018 ± 0.00018	12.0 ± 2.4
$4 < M_V < 5$	0.0029 ± 0.00029	18.0 ± 1.8
$5 < M_V < 8$	0.0072 ± 0.00072	18.5 ± 1.9
$M_V > 8$ (M dwarfs)	0.0216 ± 0.0028	18.5 ± 4.0
White dwarfs	0.0056 ± 0.001	20.0 ± 5.0
Brown dwarfs	0.0015 ± 0.0005	20.0 ± 5.0
Total	0.0889 ± 0.0071	

We also include the energy density from the smooth DM halo and a possible thin DD component. We model the bulk collisionless DM halo of the MW as a constant local density ρ_{DM} . Current measurements favor $\rho_{\text{DM}} \sim 0.01\text{--}0.02 M_{\odot}/\text{pc}^3$ at \sim kiloparsec heights above the Galactic plane [64], though we will treat ρ_{DM} as a nuisance parameter in our analysis. For the thin DD, we parametrize the density as

$$\rho_{\text{DD}}(z) = \frac{\Sigma_{\text{DD}}}{4h_{\text{DD}}} \text{sech}^2\left(\frac{z}{2h_{\text{DD}}}\right), \quad (6)$$

with Σ_{DD} and h_{DD} the DD model parameters.

Tracer stars.—For our analysis, we select TGAS stars within a cylinder about the Sun with radius $R_{\text{max}} = 150$ pc and which extends 200 pc above and below the Galactic plane. This ensures that we are within the regime of validity for several key assumptions made above: that the tilt term is negligible, that the various mass components have constant velocity dispersions, and that the radial and vertical motions are separable. Indeed, Ref. [58] showed in simulations and with data that these assumptions are satisfied within the $z \sim 200$ pc half-mass height of the disk. We also restrict to regions of the sky with average parallax uncertainties of 0.4 microarcseconds (mas) or less in our sample volume. In the Supplemental Material [65] we explore the effects of different cuts and sample volumes.

Within the spatial cuts outlined above, the TGAS sample is not complete. To account for this, we use the results of Ref. [75], which compared the TGAS catalog counts to those of the *Two Micron All-Sky Survey* catalog [76] in order to determine the effective completeness as a function of position, color, and magnitude. When taking the effective volume completeness into account, the tracer counts yield an optimal estimator for the true density with Poisson-distributed uncertainties [75].

Using the color cuts defined in Ref. [77], we consider main sequence stars of spectral types A0–G4. Later spectral types have density profiles that are closer to constant in our volume and thus less constraining. In total, our sample contains 1599 A stars, 16 302 F stars, and 14 252 early G stars, as compared with ~ 2000 stars that were used in the analysis of Ref. [51]. When including a three-dimensional model of dust in the selection function, Ref. [75] found that the difference in stellar density distributions is typically 1%–2% for a similar sample volume. We conservatively include a 3% systematic uncertainty on the density in each z bin, which also includes uncertainties in the selection function as estimated in Ref. [75]. We show the profile of our tracer stars in Fig. 1 with statistical and systematic uncertainties.

To determine the tracers’ velocity distributions at the midplane $f_{i,0}$, we project proper and radial motions along the vertical direction as $v_z = v_{z,0} + (\mu_b \kappa \cos b) / \tilde{\pi} + v_r \sin b$, where $v_{z,0}$ is the vertical velocity of the Sun, μ_b is the proper motion in Galactic latitude b in mas/yr, $\kappa = 4.74$ is a

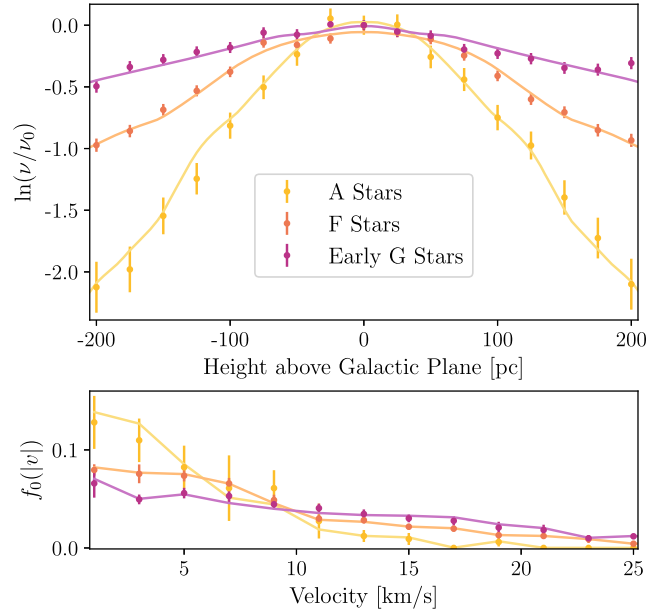


FIG. 1. The measured number density profiles (top) and velocity distributions (bottom) for the tracer stars in our sample volume, subdivided by spectral type. The solid lines are the best fit from our analysis, assuming no DD.

prefactor that converts this term to units of km/s, $\tilde{\pi}$ is the parallax in mas, and v_r is the radial velocity in km/s. Since the TGAS catalog does not have complete radial velocities, we perform a latitude cut $|b| < 5^\circ$, which geometrically ensures that radial velocities are subdominant in projecting for v_z . We then take v_r to be the mean radial velocity, $\langle v_r \rangle = -v_{x,0} \cos l \cos b - v_{y,0} \sin l \cos b - v_{z,0} \sin b$, where l is the Galactic longitude and where $v_{x,0} = 11.1 \pm 0.7^{\text{stat}} \pm 1.0^{\text{sys}}$ km/s and $v_{y,0} = 12.24 \pm 0.47^{\text{stat}} \pm 2.0^{\text{sys}}$ km/s capture the proper motion of the Sun inside the disk [78]. The midplane velocity distribution of our tracers is shown in the lower panel of Fig. 1 with combined statistical and systematic uncertainties, which are discussed further in the Supplemental Material [65].

Out-of-equilibrium effects.—A key assumption of our analysis is that the Galactic disk is locally in equilibrium. However, there are observations that suggest the presence of out-of-equilibrium features, such as bulk velocities, asymmetric density profiles about the Galactic plane, breathing density modes, and vertical offsets between populations [79–82]. Such features could also be present in the DM components. While these effects are typically manifest higher above the Galactic plane than what we consider, it is still important to account for the possibility that the disk is not in equilibrium.

However, our tracer samples appear to obey the criteria for an equilibrium disk. When adjusting for the height of the Sun above the Galactic plane (which we find to be -1.3 ± 4.6 pc, consistent with Refs. [75,83]), we do not find any significant asymmetry in the density profile above

and below the Galactic plane. We find no significant difference in the vertical velocity distribution function above and below the Galactic plane, unlike Ref. [84] which claimed evidence for a contracting mode. We also find that the midplane velocity distribution function is symmetric about $v = 0$ (we find the vertical Solar velocity $w_0 = 6.8 \pm 0.2$ km/s, consistent with the measurement of Ref. [78]) and has the expected Gaussian profile of a static isothermal population [85].

Our treatment differs from the out-of-equilibrium analysis of Ref. [51], which evolves the *observed* tracer density profile as it oscillates up and down through the spatially fixed potential of other mass components (including a DD), while determining the error on this evolution through bootstrapping. This results in a band of possible tracer profiles that could be caused by a DD in the presence of disequilibria. In contrast, our approach treats all the data on equal footing. Since changing $f_0(v)$ can potentially mimic the pinching effect from a DD, our analysis accounts for the possibility that pinching arises from fluctuations or systematics in $f_0(v)$. Thus, our analysis also scans over an analogous band of tracer profiles.

We perform a final consistency check by breaking down our tracer sample into subpopulations with different velocity dispersions, which are affected differently by disequilibria due to their different mixing timescales. In the presence of out-of-equilibrium features, separate analyses of these different subpopulations could yield discrepant parameters [86]. As detailed in the Supplemental Material [65], however, we find broad agreement between the subpopulations.

Likelihood analysis.—We search for evidence of a thin DD by combining the model and data sets described above with a likelihood function. Here we summarize our statistical analysis, which is described in full in the Supplemental Material [65].

The predicted z distribution of stars is a function of the DD model parameters (namely, the DD scale height and surface density) and nuisance parameters, which consist of (i) the 12 baryonic densities in Table I, along with their velocity dispersions, (ii) the local DM density in the halo ρ_{DM} , (iii) the height of the Sun, and (iv) the midplane stellar velocity distribution $f_0(v_j)$, where j indexes the velocity bins.

The velocity distributions are given Gaussian priors in each velocity bin with central values and widths, as shown in Fig. 1. The baryon densities and velocity dispersions are also given Gaussian priors with the parameters in Table I. The height of the Sun above the disk and local DM density are given linear priors that encompass a broad range of previous measurements, $z_{\text{sun}} \in [-30, 30]$ pc and $\rho_{\text{DM}} \in [0, 0.06] M_{\odot}/\text{pc}^3$ [64,75,83,87,88]. When combining stellar populations, we use a shared mass model but compute the densities of the *A*, *F*, and *G* stars independently and give their velocity distributions independent nuisance parameters. In analyzing all three stellar populations, we have 89 nuisance parameters.

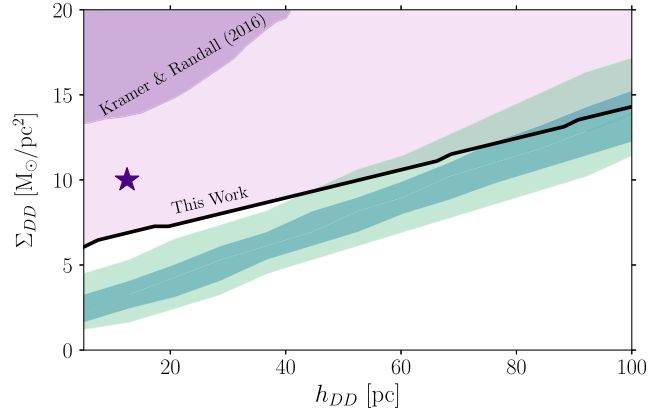


FIG. 2. The 95% constraint on the DD surface density Σ_{DD} as a function of the scale height h_{DD} , as found in this Letter and in Kramer and Randall [51]. The star indicates fiducial DD parameters that can account for phenomena such as periodic comet impacts [36]. Also shown is a comparison of the limit to the 68% and 95% containment regions (in dark and light green, respectively) on the expected limit from simulated data generated under the null hypothesis of no DD.

For fixed h_{DD} , we compute likelihood profiles as functions of Σ_{DD} by profiling over the nuisance parameters. From the likelihood profiles, we compute the 95% one-sided limit on Σ_{DD} , which is shown in Fig. 2. We also compare our limit to the expectation under the null hypothesis, which is generated by analyzing multiple simulated TGAS data sets, where we assume the fiducial baryonic mass model and include $\rho_{\text{DM}} = 0.014 M_{\odot}/\text{pc}^3$. We present the 68% and 95% containment region for the expected limits at each h_{DD} value. The TGAS limit is consistent with the Monte Carlo expectations at high h_{DD} but becomes weaker at low h_{DD} . This deviation is also manifest in the test statistic (TS), which is defined as twice the difference in log-likelihood between the maximum-likelihood DD model and the null hypothesis. We find $\text{TS} \sim 5$ at $h_{\text{DD}} \sim 5$ pc and $\Sigma_{\text{DD}} \sim 4 M_{\odot}/\text{pc}^2$; while this does indicate that the best-fit point has a nonzero DD density, the TS is not statistically significant. Moreover, we cannot exclude the possibility that the true evidence in favor of the DD is much lower due to the possible existence of systematic uncertainties that are not captured by our analysis.

The model without the thin DD provides insight into the baryonic mass model and the local properties of the bulk DM halo. While the DD limits described above were computed in a frequentist framework, we analyze the model without a DD within a Bayesian framework for the purposes of parameter estimation and model comparison. The marginalized Bayesian posterior values for the total baryonic density and local DM density are given in Table II for analyses considering the three stellar populations in isolation. Despite only analyzing data in a small sample volume, we find mild evidence in favor of halo

TABLE II. Posteriors on the total baryonic and DM halo density at the midplane, in units of M_{\odot}/pc^3 .

Component	<i>A</i> stars	<i>F</i> stars	Early <i>G</i> stars
Baryons	$0.088^{+0.006}_{-0.006}$	$0.088^{+0.007}_{-0.007}$	$0.085^{+0.007}_{-0.006}$
DM	$0.038^{+0.012}_{-0.015}$	$0.019^{+0.012}_{-0.011}$	$0.004^{+0.01}_{-0.004}$

DM: for the model with halo DM compared to that without, the Bayes factors are ~ 8.4 and 1.9 using the *A* and *F* stars, respectively, while for early *G* stars, the Bayes factor ~ 0.4 is inconclusive.

Discussion.—The results of our analysis, shown in Fig. 2, strongly constrain the presence of a DD massive enough to account for phenomena such as periodic comet impacts. If we assume that the DD radial profile is identical to that of the baryonic disk (which need not be the case), then we can set a limit on the fraction of DM with strong dissipations. Taking the baryon scale radius $R_s = 2.15$ kpc [56], the Galactocentric radius of the Earth to be 8.3 kpc [89] and the MW halo mass to be $10^{12} M_{\odot}$ [90], then dissipative disk DM can account for at most $\sim 1\%$ of DM in the MW, for $h_{\text{DD}} \lesssim 20$ pc. Previous analyses that made this assumption found that up to $\sim 5\%$ of the DM in the MW could be in the disk [14]. DDs that are marginally allowed by our analysis are not necessarily stable as per Toomre’s criterion [46,57,91], although this depends on the collisional properties of the DM [92] and on the presence of other disk components [93,94].

For the purpose of comparing our results with previous limits, the time-dependent analysis of Ref. [51] is the most similar to this Letter: although obtained in different ways, both analyses search over a band of possible density profiles that could arise from systematic effects. Our analysis is more conservative, in that we search over multiple nuisance parameters, such as in the baryon mass model. However, we set a more stringent limit owing to the increased statistics of *Gaia* over *Hipparcos*.

Our analysis was limited by uncertainties that can be better understood with the second *Gaia* data release (DR2), which will have more proper motions, spectra for measuring line-of-sight velocities, and reduced measurement errors. The improved data will reduce the systematic uncertainty on $f_0(v)$ and the line-of-sight motions will (for the first time) allow for crucial checks on isothermality and any coupling between radial and vertical motions. Thus, the lack of evidence for local out-of-equilibrium features in DR1 can be validated with DR2.

This work has made use of data from the European Space Agency (ESA) mission *Gaia* [95], processed by the *Gaia* Data Processing and Analysis Consortium (DPAC) [96]. Funding for the DPAC has been provided by national institutions, in particular, the institutions participating in the *Gaia* Multilateral Agreement. This work made use of the

MULTINEST nested sampling package [97] through its PYTHON interface [98], the Powell minimization algorithm [99] implemented in SciPy [100], and the GAIA_TOOLS package [75].

We thank Ana Bonaca, Jo Bovy, Eric Kramer, Lina Necib, Mariangela Lisanti, Adrian Liu, Christopher McKee, Lisa Randall, Eddie Schlafly, Alexandra Shelest, and Tracy Slatyer for useful conversations pertaining to this work. We also thank the anonymous referees. We acknowledge the importance of equity and inclusion in this work and are committed to advancing such principles in our scientific communities. K. S. is supported by a National Science Foundation Graduate Research Fellowship and a Hertz Foundation Fellowship. T. L. is supported in part by the Department of Energy under Award No. DE-AC02-05CH11231 and by NSF Grant No. PHY-1316783. C. W. is partially supported by the U.S. Department of Energy under Awards No. DE-SC00012567 and No. DE-SC0013999 and partially supported by the Taiwan Top University Strategic Alliance (TUSA) Fellowship. This work was performed in part at Aspen Center for Physics, which is supported by NSF Grant No. PHY-1607611.

*kschutz@berkeley.edu

- [1] N. Arkani-Hamed, D. P. Finkbeiner, T. R. Slatyer, and N. Weiner, *Phys. Rev. D* **79**, 015014 (2009).
- [2] D. E. Kaplan, G. Z. Krnjaic, K. R. Rehermann, and C. M. Wells, *J. Cosmol. Astropart. Phys.* **05** (2010) 021.
- [3] D. E. Kaplan, M. A. Luty, and K. M. Zurek, *Phys. Rev. D* **79**, 115016 (2009).
- [4] D. S. M. Alves, S. R. Behbahani, P. Schuster, and J. G. Wacker, *Phys. Lett. B* **692**, 323 (2010).
- [5] J. M. Cline, Z. Liu, and W. Xue, *Phys. Rev. D* **85**, 101302 (2012).
- [6] J. M. Cline, Z. Liu, G. D. Moore, and W. Xue, *Phys. Rev. D* **90**, 015023 (2014).
- [7] R. Foot, *Int. J. Mod. Phys. A* **29**, 1430013 (2014).
- [8] J. F. Cherry, A. Friedland, and I. M. Shoemaker, [arXiv:1411.1071](https://arxiv.org/abs/1411.1071).
- [9] Y. Hochberg, E. Kuflik, T. Volansky, and J. G. Wacker, *Phys. Rev. Lett.* **113**, 171301 (2014).
- [10] M. A. Buen-Abad, G. Marques-Tavares, and M. Schmaltz, *Phys. Rev. D* **92**, 023531 (2015).
- [11] S. Tulin, H.-B. Yu, and K. M. Zurek, *Phys. Rev. D* **87**, 115007 (2013).
- [12] S. Tulin and H.-B. Yu, *Phys. Rep.* **730**, 1 (2018).
- [13] L. Randall, J. Scholtz, and J. Unwin, *Mon. Not. R. Astron. Soc.* **467**, 1515 (2017).
- [14] J. J. Fan, A. Katz, L. Randall, and M. Reece, *Phys. Rev. Lett.* **110**, 211302 (2013).
- [15] J. Fan, A. Katz, L. Randall, and M. Reece, *Phys. Dark Universe* **2**, 139 (2013).
- [16] P. Agrawal, F.-Y. Cyr-Racine, L. Randall, and J. Scholtz, *J. Cosmol. Astropart. Phys.* **08** (2017) 021.
- [17] T. Prusti *et al.* (Gaia Collaboration), *Astron. Astrophys.* **595**, A1 (2016).

- [18] A. G. A. Brown, A. Vallenari, T. Prusti, J. H. J. de Bruijne, F. Mignard, R. Drimmel, C. Babusiaux, C. A. L. Bailer-Jones, U. Bastian *et al.* (Gaia Collaboration), *Astron. Astrophys.* **595**, A2 (2016).
- [19] F.-Y. Cyr-Racine, R. de Putter, A. Raccanelli, and K. Sigurdson, *Phys. Rev. D* **89**, 063517 (2014).
- [20] D. Harvey, R. Massey, T. Kitching, A. Taylor, and E. Tittley, *Science* **347**, 1462 (2015).
- [21] R. Massey *et al.*, *Mon. Not. R. Astron. Soc.* **449**, 3393 (2015).
- [22] F. Kahlhoefer, K. Schmidt-Hoberg, J. Kummer, and S. Sarkar, *Mon. Not. R. Astron. Soc.* **452**, L54 (2015).
- [23] Z. Chacko, Y. Cui, S. Hong, T. Okui, and Y. Tsai, *J. High Energy Phys.* **12** (2016) 108.
- [24] W. Fischler, D. Lorshbough, and W. Tangarife, *Phys. Rev. D* **91**, 025010 (2015).
- [25] M. Raveri, W. Hu, T. Hoffman, and L.-T. Wang, *Phys. Rev. D* **96**, 103501 (2017).
- [26] R. Foot, *Phys. Rev. D* **88**, 023520 (2013).
- [27] K. Petraki, L. Pearce, and A. Kusenko, *J. Cosmol. Astropart. Phys.* **07** (2014) 039.
- [28] E. Rosenberg and J. Fan, *Phys. Rev. D* **96**, 123001 (2017).
- [29] R. Foot and S. Vagnozzi, *J. Cosmol. Astropart. Phys.* **07** (2016) 013.
- [30] F.-Y. Cyr-Racine and K. Sigurdson, *Phys. Rev. D* **87**, 103515 (2013).
- [31] K. Schutz and T. R. Slatyer, *J. Cosmol. Astropart. Phys.* **01** (2015) 021.
- [32] K. K. Boddy, M. Kaplinghat, A. Kwa, and A. H. G. Peter, *Phys. Rev. D* **94**, 123017 (2016).
- [33] J. M. Cline, Z. Liu, G. D. Moore, and W. Xue, *Phys. Rev. D* **89**, 043514 (2014).
- [34] A. Das and B. Dasgupta, *Phys. Rev. D* **97**, 023002 (2018).
- [35] M. R. Buckley and A. DiFranzo, *Phys. Rev. Lett.* **120**, 051102 (2018).
- [36] L. Randall and M. Reece, *Phys. Rev. Lett.* **112**, 161301 (2014).
- [37] L. Randall and J. Scholtz, *J. Cosmol. Astropart. Phys.* **09** (2015) 057.
- [38] R. Foot and Z. K. Silagadze, *Phys. Dark Universe* **2**, 163 (2013).
- [39] P. Agrawal and L. Randall, *J. Cosmol. Astropart. Phys.* **12** (2017) 019.
- [40] S. K. Lee, M. Lisanti, B. R. Safdi, T. R. Slatyer, and W. Xue, *Phys. Rev. Lett.* **116**, 051103 (2016).
- [41] A. Caputo, J. Zavala, and D. Blas, *Phys. Dark Universe* **19**, 1 (2018).
- [42] G. D'Amico, P. Panci, A. Lupi, S. Bovino, and J. Silk, *Mon. Not. R. Astron. Soc.* **473**, 328 (2018).
- [43] M. McCullough and L. Randall, *J. Cosmol. Astropart. Phys.* **10** (2013) 058.
- [44] J. Fan, A. Katz, and J. Shelton, *J. Cosmol. Astropart. Phys.* **06** (2014) 059.
- [45] E. D. Kramer and M. Rowan, arXiv:1610.04239.
- [46] N. J. Shaviv, arXiv:1606.02851.
- [47] L. Lindegren *et al.*, *Astron. Astrophys.* **595**, A4 (2016).
- [48] D. Michalik, L. Lindegren, and D. Hobbs, *Astron. Astrophys.* **574**, A115 (2015).
- [49] E. Høg, C. Fabricius, V. V. Makarov, S. Urban, T. Corbin, G. Wycoff, U. Bastian, P. Schwekendiek, and A. Wicenc, *Astron. Astrophys.* **355**, L27 (2000).
- [50] M. A. C. Perryman *et al.*, *Astron. Astrophys.* **323**, L49 (1997).
- [51] E. D. Kramer and L. Randall, *Astrophys. J.* **824**, 116 (2016).
- [52] J. Holmberg and C. Flynn, *Mon. Not. R. Astron. Soc.* **313**, 209 (2000).
- [53] K. Kuijken and G. Gilmore, *Mon. Not. R. Astron. Soc.* **239**, 605 (1989).
- [54] K. Kuijken and G. Gilmore, *Astrophys. J. Lett.* **367**, L9 (1991).
- [55] K. Kuijken and G. Gilmore, *Mon. Not. R. Astron. Soc.* **239**, 571 (1989).
- [56] J. Bovy and H.-W. Rix, *Astrophys. J.* **779**, 115 (2013).
- [57] C. F. McKee, A. Parravano, and D. J. Hollenbach, *Astrophys. J.* **814**, 13 (2015).
- [58] S. Garbari, J. I. Read, and G. Lake, *Mon. Not. R. Astron. Soc.* **416**, 2318 (2011).
- [59] J. N. Bahcall, *Astrophys. J.* **276**, 169 (1984).
- [60] J. Bovy, *Mon. Not. R. Astron. Soc.* **468**, L63 (2017).
- [61] H. Silverwood, S. Sivertsson, P. Steger, J. I. Read, and G. Bertone, *Mon. Not. R. Astron. Soc.* **459**, 4191 (2016).
- [62] E. D. Kramer and L. Randall, *Astrophys. J.* **829**, 126 (2016).
- [63] C. Flynn, J. Holmberg, L. Portinari, B. Fuchs, and H. Jahreiss, *Mon. Not. R. Astron. Soc.* **372**, 1149 (2006).
- [64] J. I. Read, *J. Phys. G* **41**, 063101 (2014).
- [65] See Supplemental Material at <http://link.aps.org/supplemental/10.1103/PhysRevLett.121.081101>, which includes Refs. [66–74], for details regarding data selection and quality cuts, validation of the analysis using mock data, extended results, and discussion of the statistical methods and astrophysical interpretation.
- [66] L. Anderson, D. W. Hogg, B. Leistedt, A. M. Price-Whelan, and J. Bovy, arXiv:1706.05055.
- [67] P. J. McMillan, G. Kordopatis, A. Kunder, J. Binney, J. Wojno, T. Zwitter, M. Steinmetz, J. Bland-Hawthorn, B. K. Gibson, G. Gilmore, E. K. Grebel, A. Helmi, U. Munari, J. F. Navarro, Q. A. Parker, G. Seabroke, and R. F. G. Wyse, *Mon. Not. R. Astron. Soc.* **477**, 5279 (2018).
- [68] J. Bovy, D. Kawata, and J. A. S. Hunt, *Mon. Not. R. Astron. Soc.* **473**, 2288 (2018).
- [69] S. Pasetto, E. K. Grebel, T. Zwitter, C. Chiosi, G. Bertelli, O. Bienayme, G. Seabroke, J. Bland-Hawthorn, C. Boeche, B. K. Gibson, G. Gilmore, U. Munari, J. F. Navarro, Q. Parker, W. Reid, A. Silviero, and M. Steinmetz, *Astron. Astrophys.* **547**, A71 (2012).
- [70] G. Monari, B. Famaey, and A. Siebert, *Mon. Not. R. Astron. Soc.* **452**, 747 (2015).
- [71] L. Zhang, H.-W. Rix, G. van de Ven, J. Bovy, C. Liu, and G. Zhao, *Astrophys. J.* **772**, 108 (2013).
- [72] S. Garbari, C. Liu, J. I. Read, and G. Lake, *Mon. Not. R. Astron. Soc.* **425**, 1445 (2012).
- [73] J. Bovy and S. Tremaine, *Astrophys. J.* **756**, 89 (2012).
- [74] G. Cowan, K. Cranmer, E. Gross, and O. Vitells, *Eur. Phys. J. C* **71**, 1554 (2011); **73**, 2501(E) (2013).
- [75] J. Bovy, *Mon. Not. R. Astron. Soc.* **470**, 1360 (2017).
- [76] M. F. Skrutskie *et al.*, *Astron. J.* **131**, 1163 (2006).
- [77] M. J. Pecaut and E. E. Mamajek, *Astrophys. J. Suppl. Ser.* **208**, 9 (2013).

- [78] R. Schönrich, J. Binney, and W. Dehnen, *Mon. Not. R. Astron. Soc.* **403**, 1829 (2010).
- [79] L. M. Widrow, S. Gardner, B. Yanny, S. Dodelson, and H.-Y. Chen, *Astrophys. J.* **750**, L41 (2012).
- [80] M. E. K. Williams *et al.*, *Mon. Not. R. Astron. Soc.* **436**, 101 (2013).
- [81] J. L. Carlin *et al.*, *Astrophys. J.* **777**, L5 (2013).
- [82] B. Yanny and S. Gardner, *Astrophys. J.* **777**, 91 (2013).
- [83] J. Holmberg, C. Flynn, and L. Lindegren, in *Hipparcos—Venice '97*, ESA Special Publication, edited by R. M. Bonnet, E. Høg, P. L. Bernacca, L. Emiliani, A. Blaauw, C. Turon, J. Kovalevsky, L. Lindegren, H. Hassan, M. Bouffard, B. Strim, D. Heger, M. A. C. Perryman, and L. Woltjer (1997), Vol. 402, p. 721, <http://adsabs.harvard.edu/abs/1997ESASP.402..721H>.
- [84] N. J. Shaviv, [arXiv:1606.02595](https://arxiv.org/abs/1606.02595).
- [85] J. Binney and S. Tremaine, *Galactic Dynamics* (Princeton University Press, Princeton, NJ, 2011).
- [86] N. Banik, L. M. Widrow, and S. Dodelson, *Mon. Not. R. Astron. Soc.* **464**, 3775 (2017).
- [87] Y. C. Joshi, *Mon. Not. R. Astron. Soc.* **378**, 768 (2007).
- [88] D. J. Majaess, D. G. Turner, and D. J. Lane, *Mon. Not. R. Astron. Soc.* **398**, 263 (2009).
- [89] S. Gillessen, P. M. Plewa, F. Eisenhauer, R. Sari, I. Waisberg, M. Habibi, O. Pfuhl, E. George, J. Dexter, S. von Fellenberg, T. Ott, and R. Genzel, *Astrophys. J.* **837**, 30 (2017).
- [90] P. J. McMillan, *Mon. Not. R. Astron. Soc.* **465**, 76 (2017).
- [91] A. Toomre, *Astrophys. J.* **139**, 1217 (1964).
- [92] W. J. Quirk, *Astrophys. J.* **176**, L9 (1972).
- [93] R. R. Rafikov, *Mon. Not. R. Astron. Soc.* **323**, 445 (2001).
- [94] C. J. Jog, [arXiv:1308.1754](https://arxiv.org/abs/1308.1754).
- [95] <https://www.cosmos.esa.int/gaia>.
- [96] <https://www.cosmos.esa.int/web/gaia/dpac/consortium>.
- [97] J. Buchner, A. Georgakakis, K. Nandra, L. Hsu, C. Rangel, M. Brightman, A. Merloni, M. Salvato, J. Donley, and D. Kocevski, *Astron. Astrophys.* **564**, A125 (2014).
- [98] J. Buchner, A. Georgakakis, K. Nandra, L. Hsu, C. Rangel, M. Brightman, A. Merloni, M. Salvato, J. Donley, and D. Kocevski, *Astron. Astrophys.* **564**, A125 (2014).
- [99] M. J. Powell, *Comput. J.* **7**, 155 (1964).
- [100] E. Jones, T. Oliphant, P. Peterson *et al.* (2001), <http://www.citeulike.org/group/19049/article/13344001>.